AIAA AVIATION Forum
June 25-29, 2018, Atlanta, Georgia
2018 AIAA/CEAS Aeroacoustics Conference

10.2514/6.2018-3614



# Comparison of Noise from High-Performance Military Aircraft for Ground Run-up and Flyover Operations

Brent Reichman,[1] Kent L. Gee,[2] Tracianne B. Neilsen,[3] and S. Hales Swift[4]
*Brigham Young University, Provo, UT, 84602*

Alan T. Wall[5]
*Air Force Research Laboratory, Wright-Patterson Air Force Base, OH, 45433*

and

J. Micah Downing[6] and Michael M. James[7]
*Blue Ridge Research and Consulting, LLC, Asheville, NC 28801*



**While the majority of jet noise analysis takes place with a static jet or aircraft, airbase and community military jet noise exposure happens for the most part when the aircraft is in flight. Comparisons between flyover and ground run-up measurements for high-performance military aircraft have not been previously published. This paper presents comparisons between static ground run-up and flyover measurements for the F-35 operating at 150% Engine Thrust Request. The overall sound pressure levels and spectra are shown for the two scenarios, as well as indicators of nonlinear propagation and shock content, specifically the derivative skewness and average steepening factor. The overall sound pressure level is reduced in the peak radiation direction aft of the aircraft but increased in the forward direction. The peak frequency of the noise is relatively unaffected by flight effects, though the amplitude of each frequency may vary. The increase in level in the forward direction results in shock formation that is absent during ground run-up measurements.**

## Nomenclature

ETR = engine thrust request
MARP = microphone array reference point
OASPL = overall sound pressure level, dB re 20 $\mu$Pa
OTO = one-third octave

## I. Introduction

While the majority of jet noise research occurs with a static jet or aircraft, in-flight operations represent the majority of jet noise exposure from a community noise standpoint. Static measurements, either from model-scale jets or tethered aircraft, provide for a controlled environment with set locations and long exposure times. In-flight measurements are inherently complicated by factors such as smaller integration time for metrics, uncertainty in distances between the aircraft and measurement locations, and atmospheric propagation effects [1,2]. However, the changing nature of the source between static and in-flight operations necessitates measurements during flyover events.

[1]Ph.D. Candidate, Dept. of Physics and Astronomy, N283 ESC, AIAA Student Member.
[2]Professor, Dept. of Physics and Astronomy, N283 ESC, AIAA Senior Member.
[3]Associate Professor, Dept. of Physics and Astronomy, N283 ESC, AIAA Member.
[4]Postdoctoral Fellow, Dept. of Physics and Astronomy, N283 ESC, AIAA Member.
[5]Research Physicist, Battlespace Acoustics Branch, Air Force Research Laboratory, 2610 Seventh St., Bldg. 441, Wright-Patterson AFB, OH 45433, AIAA Member.
[6] President and Chief Scientist, 29 N Market St, Suite 700, AIAA Member.
[7] Sr. Vice President and Chief Engineer, 29 N Market St, Suite 700, AIAA Member.

Jet noise can be ascribed to several different phenomena, but the dominant structure in military jet aircraft noise is caused by the turbulent mixing of the jet with the air around it. Analytical derivations and measurements of in-flight effects have shown how the turbulent mixing region is affected by a secondary flow [3,4]. Changes include a smaller relative jet velocity and a lengthening of the potential core, which result in three main changes: first, the overall sound pressure level (OASPL) is reduced in the maximum radiation region. Second, the peak radiation direction is shifted forward. Third, the OASPL increases in the forward direction. These changes are confirmed through comparison with experimental results[5]. Analytically predicted OASPL values compare favorably with experiment, showing agreement within 1-2 dB for Michalke and Michel[5]. However, their prediction method relies on extended measurements of the OASPL at many known nozzle exit velocities and temperatures, limiting its application in military jet noise predictions as exact temperature and velocity conditions are not publicly available.

The change in levels associated with flight effects is likely to affect the importance of nonlinear propagation in the aircraft far field.[6] Nonlinear propagation in jet noise has been shown to steepen waveforms and form shocks in the far field, resulting in high-frequency energy that would otherwise not exist at large distances from the source.[7,8,9] The effects of nonlinear propagation have been shown in model-scale experiments [10,11,12] and full-scale military jet engine noise experiments [13,14], but the importance of nonlinear effects is especially apparent in the far field of military jet aircraft. Viswanathan and Czech [6] showed that high-frequency energy in the far field can be attributed to nonlinear propagation for laboratory-scale jets with co-flow. McInerny *et al*. [15] and Reichman *et al*. [16] showed evidence of nonlinear propagation and the presence of shocks in the far field of military jet aircraft during flyover measurements but did not compare the effects to similar conditions on the ground. Nonlinear effects are dependent on the amplitude of the noise, so changes in OASPL-reductions in the peak radiation direction and increases in the forward direction-are likely to affect the importance of nonlinear propagation in the noise in those directions.

This paper represents the first comparison of in-flight noise radiation with that from static or ground run-up measurements for military jet aircraft. This paper compares OASPL, spectra, and various nonlinearity indicators to show that even for exit velocities and aircraft speeds higher than those seen in laboratory-scale experiments, the same general trends identified by Michalke and Michel hold for static and flying military aircraft. In contrast with ground run-up measurements, evidence of azimuthal directivity is seen in flyover measurements. Flyover events are examined at 75%, 100%, and 150% ETR, and consistency of the results with aircraft height is shown. In addition, the nonlinearity analysis shows that the slight reduction in OASPL in the peak radiation direction does not significantly alter nonlinear propagation and shock content, but significant shocks are present in the forward direction during flyover measurements, a marked changed from the ground run-up measurements.

## II. Measurements

The comparisons in this paper are performed on measurements of the F-35A and F-35B variants for both ground run-up and flyover measurements. Measurements were taken in September 2013 at Edwards Air Force Base, California. The ground run-up measurement layout has already been described in detail by James *et al.* [17] but microphone locations are shown here in Figure 1(a). Each location shown here has one microphone height at each location, with heights ranging from 1.5 m to 9.1 m. The origin of the coordinate system in Figure 1(a) is the microphone array reference point (MARP), located 6.7 m downstream of the nozzle as an approximate source location, meaning the nozzle is located at $x = 6.7$ m and exhaust is flowing in the $-x$ direction. Measurements were made by a collaboration of the Air Force Research Laboratory; Blue Ridge Research and Consulting, LLC; Brigham Young University; Wyle Laboratories; and the Naval Air Systems Command (NAVAIR).

While the ground run-up measurement consisted primarily of semi-circular arcs of microphones at different radii from the MARP, the flyover array consisted of linear arrays as shown in Figure 1(b), which has been described in part by Reichman *et al*. [16]. Microphones were suspended from two cranes at a distance of 305 m on either side of the nominal flight path, at heights ranging from 0 m to 91 m. Microphones between these two cranes were arranged in a line perpendicular to the nominal flight path, and at each measurement location microphones were located at 0 m, 1.5 m, and 9.1 m. Finally, an array of microphones was located on the ground below the nominal flight path. The majority of microphones were ½" (12.7 mm), with some ¼" (6.3 mm) microphones on the crane at $y = 305$ m. Sampling rates varied between measurement systems, with sampling rates of 96, 192, and 204.8 kHz. For the flyover events used in this study the aircraft flew in the $+x$ direction nearly over the $y = 0$ line, within 10 m, at a height of 115 m. Data from the aircraft were used to ensure that analyses were performed only for the times at which the aircraft was operating at the desired engine condition.

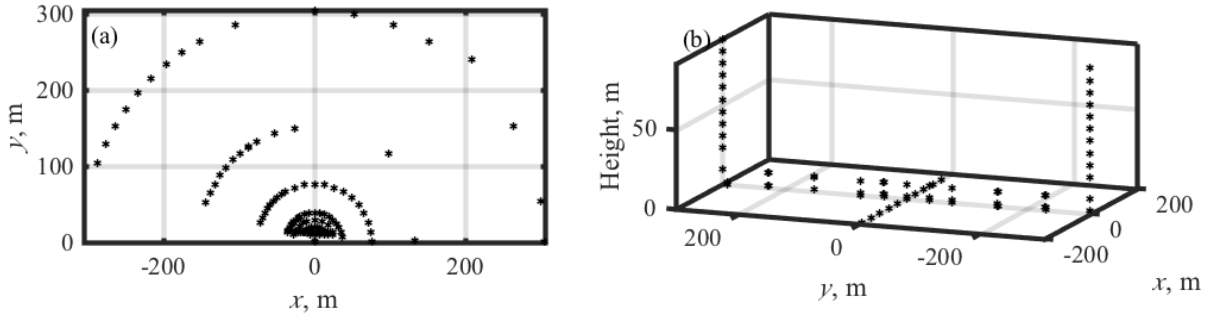


**Figure 1. Layout for the (a) ground run-up and (b) flyover measurements.**

Directivity of the flyover noise is discussed in both the polar and azimuthal directions. As is typical in reporting jet noise, the polar angle $\theta$ is measured from the nose of the aircraft as shown in Figure 2. This angle varies as the aircraft flies along the flight track for each microphone, while the azimuthal angle, $\phi$, is relatively constant. An azimuthal angle of $\phi = 0$ means that the microphone is located directly under the aircraft, while $\phi = 90$ means the microphone is located at aircraft height.

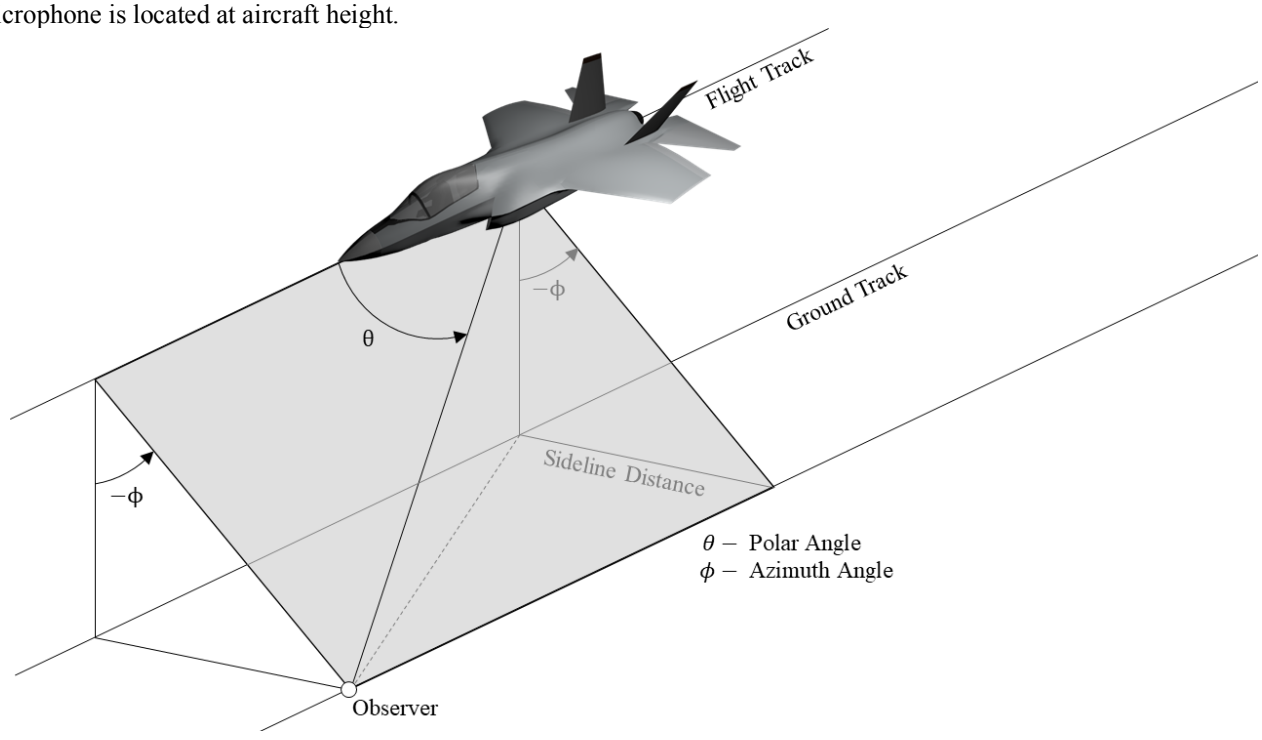


**Figure 2. Illustration of azimuthal angle $\phi$ and polar angle $\theta$ relative to the flight track.**

## III. Metrics

When comparing the sound field between ground run-up and flyover there are multiple quantities of interest. While there are many sound metrics that could be compared, this paper concentrates on sound pressure level and two nonlinearity metrics, the derivative skewness and ASF.

### A. Sound pressure level

Sound pressure level is the simplest quantity that can be compared between these situations, as it can be adjusted for spherical spreading. Comparisons are slightly more complicated when performed frequency-by-frequency, as atmospheric absorption and nonlinear propagation complicate distance corrections, in particular for higher frequencies and over long distances.[11] However, a comparison as a function of OTO band center frequency can still be made because of the wide range of measurement locations in both ground run-up and flyover measurements.

### B. Derivative Skewness

The skewness of a distribution expresses asymmetry of the PDF and accentuates outliers due to the cubed nature of the numerator. The skewness of a zero-mean variable $x$ is defined as

$$\mathrm{Sk}\{x\} = \frac{E[x^3]}{E[x^2]^{\frac{3}{2}}}. \tag{1}$$

A value of $\mathrm{Sk}\{x\} = 0$ represents a symmetric distribution, while a positive number indicates the presence of a greater number of large positive values than negative. The skewness of the pressure waveform, $\mathrm{Sk}\{p\}$ was initially used to quantify crackle, an auditory phenomenon associated with shock waves within jet noise.[13] However, to quantify shocks themselves it is more useful to use the derivative skewness, $\mathrm{Sk}\{\partial p/\partial t\}$, which refers to the skewness of the PDF of the first time derivative of the waveform and expresses an asymmetry in derivative values. The derivative skewness accentuates the large derivatives (rapid pressure increases) associated with shock waves, thus, is a useful indicator of shocks forming due to nonlinear propagation.[18,19] It has been shown that a derivative skewness value greater than five is indicative of significant shocks within a waveform.[20,21]

### C. ASF

The ASF [22] is also based on derivative values and defined as the average value of the positive derivatives over the average value of the negative derivatives:

$$\mathrm{ASF}\{p\} = \frac{E[\dot{p}^+]}{E[\dot{p}^-]}. \tag{2}$$

The ASF, which is an inverse of the previously used WSF [23], is a linear average of derivative values, which makes it less sensitive to outliers than the derivative skewness, and thus better represents average behavior. An ASF value of one represents a waveform with no significant steepening, while $\mathrm{ASF} > 1$ represents some steepening. It has been shown that for jet noise, both full-scale and model-scale, that an ASF value between 1.5 and 2 is indicative of the presence of shocks, with an ASF value approaching two suggesting significant shock content.[24,25]

### D. Example of flyover metrics

To show expected behavior in metrics during a flyover event, an example waveform and the calculated metrics are shown in Figure 3. The waveform, which was recorded at a microphone located at $x = 0, y = 0, z = 0$ in Figure 1(b), is shown in Figure 3(a) along with its derivative in Figure 3(b), with $t = 0$ corresponding to the time of peak OASPL. Using tracking data from the aircraft, the relative position of the aircraft to the microphone in question can be calculated as a function of time; the time-dependent distance, $r(t)$, and polar angle, $\theta(t)$, are shown in Figure 3(c). To describe the time-varying properties of the sound, metrics were calculated for 0.1 s sections of the waveform. Each section contained 50% overlap, meaning that the resolution is 0.05 s. The resulting 0.1 sec OASPL, derivative skewness and ASF are shown in Figure 3(d)-(f), respectively.

The aircraft passes nearest the microphone shortly before the peak OASPL, at $t = -0.35$ s. The derivative skewness in Figure 3(e) peaks at the same time as the OASPL ($t = 0$), but another peak is seen at $t = -0.9$ s,

indicating that shocks are present in the forward direction of the aircraft. These forward shocks, which produce a noticeable effect in auralizations, are the predominant feature shaping the ASF, which peaks at $t = -1.2$ s. It is important to note that the distance to the aircraft is not constant over the duration of the flight, making it difficult to compare the ASF and derivative skewness values as a function of angle at a single microphone.

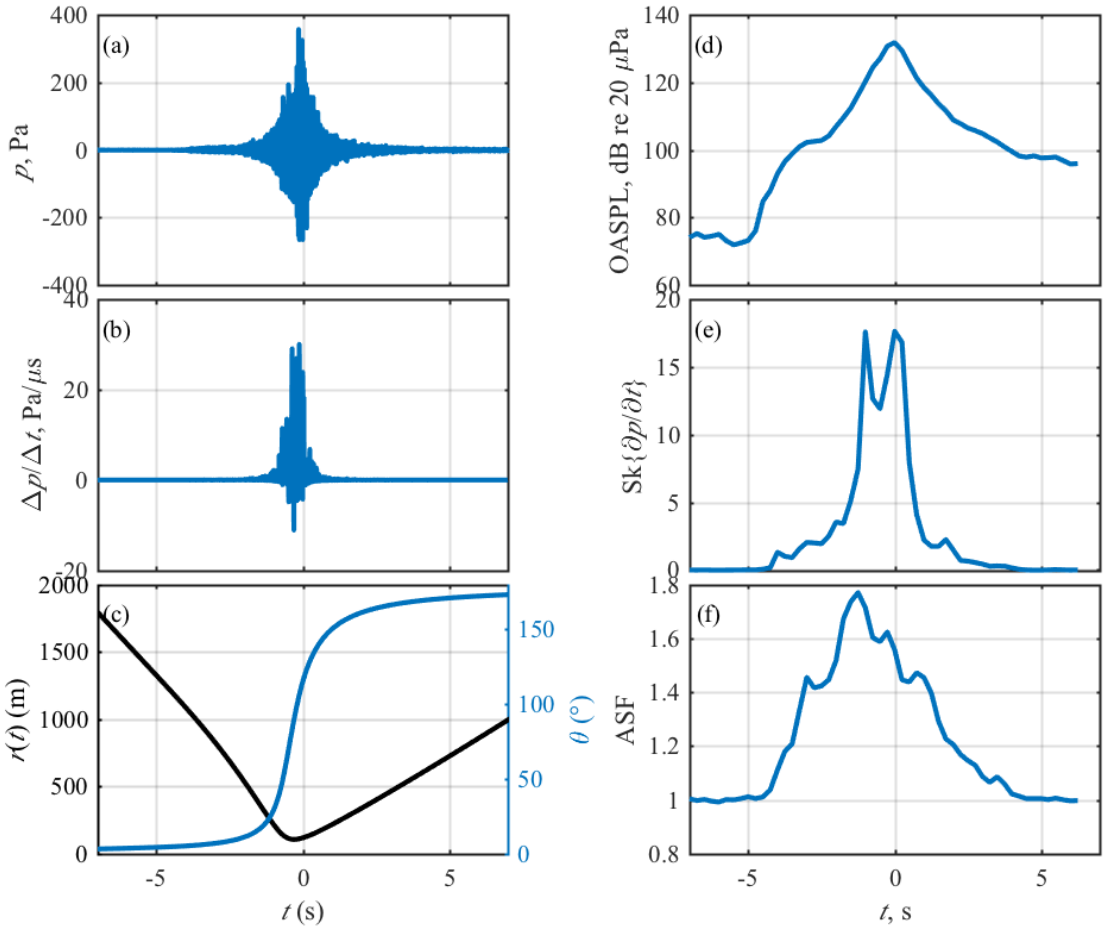


**Figure 3. Example waveform and metrics from a flyover measurement.**

## IV. OASPL Comparison

Comparisons of OASPL and directivity of the source between ground run-up and flyover measurements have been made in previous experiments [3,5,26,27,28], and the subject has received an analytical treatment from Michalke and Michel [3]. As explained earlier, the three main consequences expected are (1) a decrease in OASPL in the main directivity lobe, (2) a shift towards the sideline in the main directivity lobe, and (3) an increase in OASPL in the forward direction. In this section directivity curves from flyover measurements are compared with those from ground run-up. Expected changes between the two measurements are observed, and some evidence of azimuthal variation during flyover measurements is shown.

### A. Method

To compare between ground run-up and flyover measurements, we must first find common measurement locations at which to compare. The data from the ground run-up measurements provide information at various distances and angles ranging from 0° to 160°. However, in the far field where a direct comparison with flyover measurements is more likely, the measurement locations are more sparse, with microphones located only at distances of 76 m, 152 m,

and 305 m from the MARP at spacing of 5-10°. In comparison with this, as the aircraft flies through the flyover measurement array, each microphone receives sound radiated at nearly all angles, but over a wide and constantly varying set of distances. However, because atmospheric absorption and nonlinear propagation have relatively small effects on OASPL (~1 dB) when compared with geometric spreading, the distances can be normalized to a standard distance assuming spherical spreading. This allows the OASPL curve shown in Figure 3(d) to be compared with measurements made during ground run-up at a set distance, e.g. 76 m, over a wide range of angles.

### A. Directivity curves

Normalizing the OAPSPL for distance gives a polar directivity curve for each microphone from the flyover measurement arrays. These curves are shown in Figure 4(a) for all microphones for a single flyover event, with line color corresponding to azimuthal angle $\phi$, with $\phi = 0°$ corresponding to directly underneath the aircraft, and $\phi = 90°$ corresponding to a microphone at aircraft height. Though the curves exhibit a similar pattern for $\theta =$ 10 to 160°, the variation in OASPL is on the order of 5-10 dB. This variation can come from a variety of sources, including weather effects and azimuthal angle. The ground microphones experience pressure doubling due to the hard ground at the measurement location, while elevated microphones have a mix of destructive and constructive interference. This results in the ground microphones having an OASPL roughly 3 dB higher than the elevated microphones: Thus, 3 dB is subtracted from the ground mic directivity curves before being plotted in Figure 4(a). Taking the average after this correction results in the two curves shown in Figure 4(b), where the ground and above-ground OASPL values agree closely with each other. The corrected data will be used for all subsequent data shown.

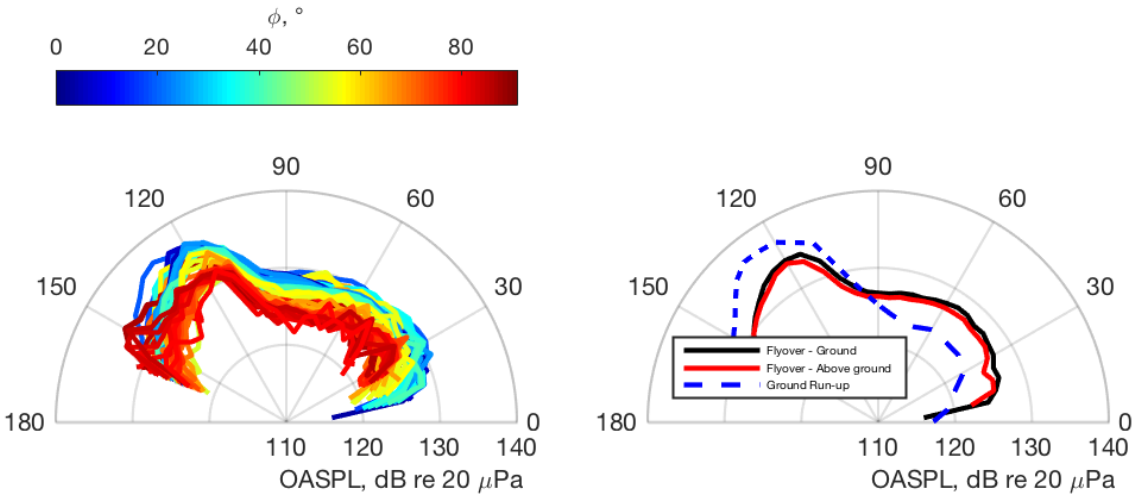


**Figure 4. Calculated directivity curves at a height of 76 m from (a) all microphone channels for one flyover event, colored according to the azimuthal angle $\phi$, and (b) the averaged result for the flyover array's ground microphones (-3 dB correction, black), the flyover array's elevated microphones (red), and the ground run-up arcs at 76m (blue).**

### B. Comparison of average results

The average behavior of the flyover directivity curves in Figure 4(a) exhibit the expected behavior from earlier work. The mean of the directivity curves for both on-ground mics and above-ground mics is shown in Figure 4(b) and compared with the ground run-up measurement. This comparison exhibits many of the trends predicted analytically by Michalke and Michel.[3] The trends predicted by Michalke and Michel include a reduction in OASPL in the flyover in the maximum radiation region, as well as a shift in the maximum radiation region in the forward direction. These trends are observed in Figure 4(b), with a peak directivity of 115° for the flyover results compared with 130° during ground run-up. In addition, Michalke and Michel also predicted an increase in OASPL in the forward direction, which is evident in Figure 4(b) as an increase of 3-4 dB is seen from 20°-90°. Though the lack of exhaust velocity and

temperature data for the F-35 prevent predictions of flyover OASPL based on ground run-up data, the trends seen in the comparison agree with other experiments and the theory set forth by Michalke and Michel.

### C. Consistency with aircraft height

The results above are consistent with expectations from prior work but represent only one flyover event. To begin investigating the consistency of the results, directivity curves are shown for a flyover event at an aircraft height of 305 m. These polar directivity curves confirm many of the features observed at the aircraft height of 76 m (Figure 4). First, the curves in Figure **5**(a) show a noticeable azimuthal directivity. While azimuthal angle is limited to ~50 degrees at this aircraft height, a decrease of ~2 dB is consistent with the difference in Figure 4. In addition, excellent agreement is seen in the OASPL between the two events, as shown in Figure 4(b) and Figure **5**(b). The exact trends seen at a height of 76 m in Figure 4(b), including a reduction in OASPL in the aft direction and an increase in the forward direction, are observed at 305 m, and levels agree at all observed angles to within 1 dB. These confirm the observation of previously reported behavior for the shift in polar directivity due to flight effects. However, they also point to an azimuthal variation not seen in laboratory-scale experiments.

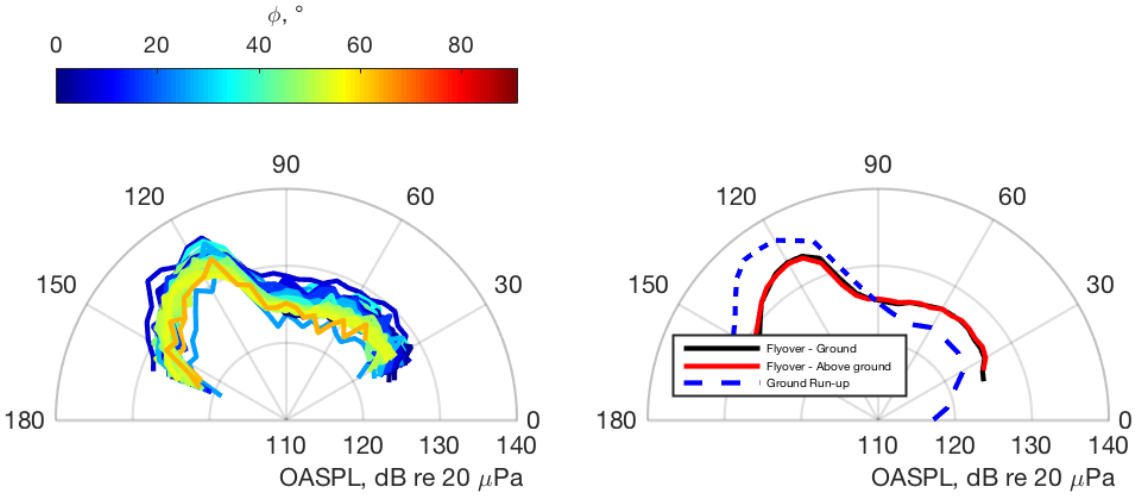


**Figure 5. Polar directivity of an aircraft at height of 305 m (a) shown for all microphones and (b) an average directivity for microphones located on and above the ground and compared with ground run-up.**

### D. Azimuthal directivity

As seen in Figure 4(a) and Figure **5**(a), differences due to azimuthal directivity during flyover events may be on the order of 3-4 dB. To investigate this possible variation, the OASPL from both flyover heights is interpolated onto a grid in $\theta$ and $\phi$, and plotted as a function of $\theta$ and $\phi$ to show azimuthal variations. The azimuthal variations are shown in Figure 6 for flyover events at (a) 76 m and (b) 305 m. It is interesting to note that the directivity maximum is not located directly under the aircraft, but roughly 20-30° to the side. A decrease in OASPL on the order of 3 dB is seen at larger angles of 70-80° in Figure 6(a). However, in Figure 6(b) these larger angles are not visible due to the increased aircraft height. While discrepancies exist between the directivity shown between the two heights, both show a decrease in OASPL for $\phi > 50 - 60°$.

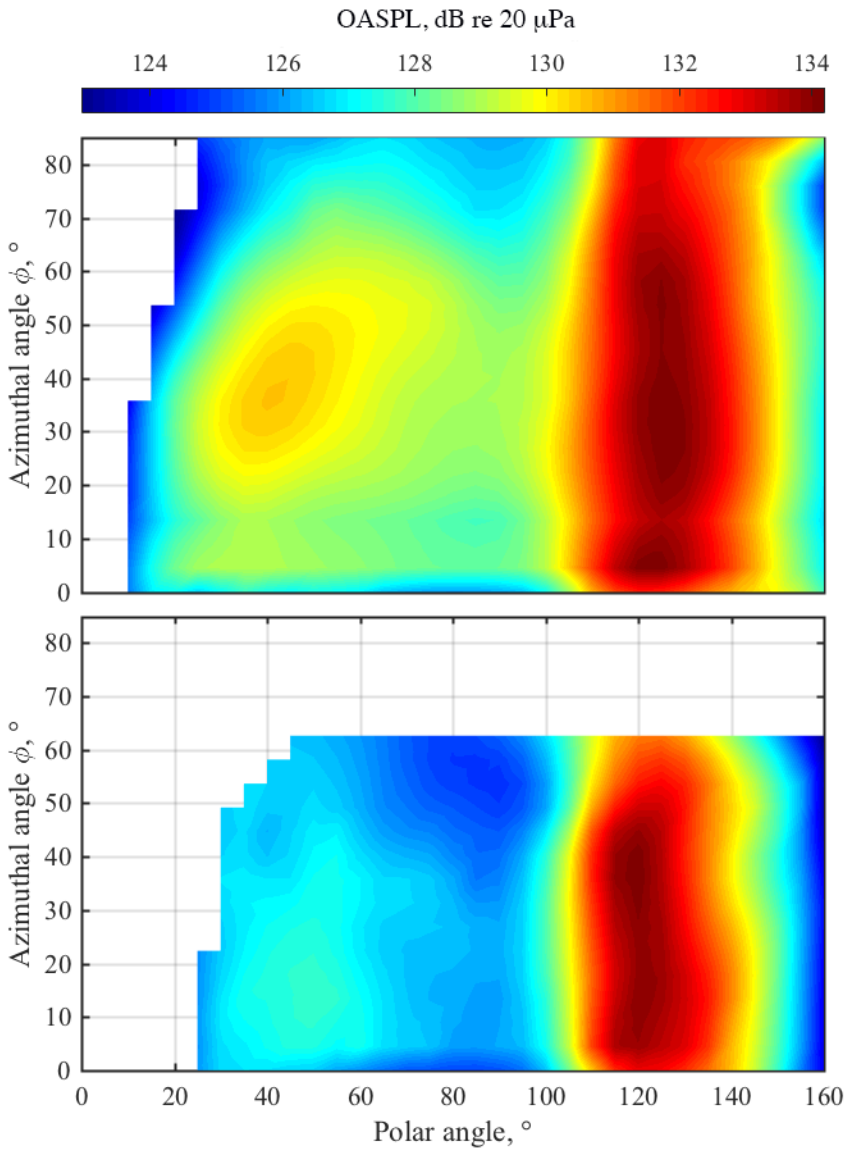


**Figure 6. OASPL as a function of polar angle $\theta$ and azimuthal angle $\phi$ during flyover events at aircraft heights of (a) 76 m and (b) 305 m.**

Because the circular nozzle of the F-35 would not suggest any azimuthal asymmetry, the azimuthal directivity seen in Figure 6 is at least in part unexpected. While factors such as flow around the aircraft and its features may produce some directivity, before differences can be attributed to azimuthal directivity other factors, such as longer propagation distances to microphones at a higher angle $\phi$, must be estimated. One simple way of calculating expected losses due to linear atmospheric absorption is to calculate $\alpha$, the expected absorption coefficient, at the characteristic frequency of the jet noise. At a frequency of 400 Hz, roughly twice the peak frequency of the noise from an F-35, the expected loss due to atmospheric absorption over a distance of 300 m is 0.65 dB, smaller than the variation with $\phi$ shown in Figure 6. Another possible explanation is loss due to nonlinear propagation, but previous modeling has shown that this effect should be limited to roughly 1 dB over the range of interest. Thus, it is likely

that the differences seen in Figure 6 are in fact due to azimuthal directivity, rather than atmospheric absorption and nonlinear propagation.

Another way of separating propagation and azimuthal effects is to consider the variation with distance at a single polar angle, as shown in Figure 7. Here the OASPL, corrected for spherical spreading to a common distance of 76 m, is shown at each microphone as a function of measurement distance $r$ for a constant polar angle of $\theta = 120°$ relative to the nose of the aircraft. The data are shown for six flyover events at 76 m and 305 m at 150% ETR in Figure 7(a) and 100% ETR in Figure 7(b), with each data point representing the OASPL at one microphone for a single flyover event. Each data point is colored according to azimuthal angle $\phi$. Clustering of the data is immediately noticeable, with the two groups of blue circles at 100 m and 400 m representing the mics closest to the flight path at the flyover heights of 76 m and 305 m. While in each group there is a wide spread of OASPL levels, the slight decrease in average behavior of the OASPL between these two groups is similar to what would normally be expected due to the longer propagation distance. In a lossless environment, these two groups should be nearly identical when corrected for spherical spreading to a common distance. Instead, a decrease of ~1.5 dB is seen when comparing average OASPL for each group. As explained above, this is likely due a combination of losses from atmospheric absorption over an additional 300 m of propagation and losses due to nonlinear propagation. A similar difference in level is seen when comparing cyan and green dots at 200 m and 450-500 m. However, the group of red and orange dots at 350 m is substantially lower than the blue dots at a similar distance. Though these two groupings are from different flyover heights, with the red dots from a flyover height of 76 m and the blue dots at a flyover height of 305 m, the propagation distances are nearly identical and long-range propagation effects should be similar. Thus, the difference between the average behavior of these two groups, on the order of 2 dB, can likely be attributed to azimuthal directivity. This behavior is not limited to a single flyover event, as the data shown here are from multiple flyover events, and the trends seen in Figure 7(a) for 150% ETR are also observed in Figure 7(b) at 100% ETR, showing systematic asymmetry in the azimuthal direction.

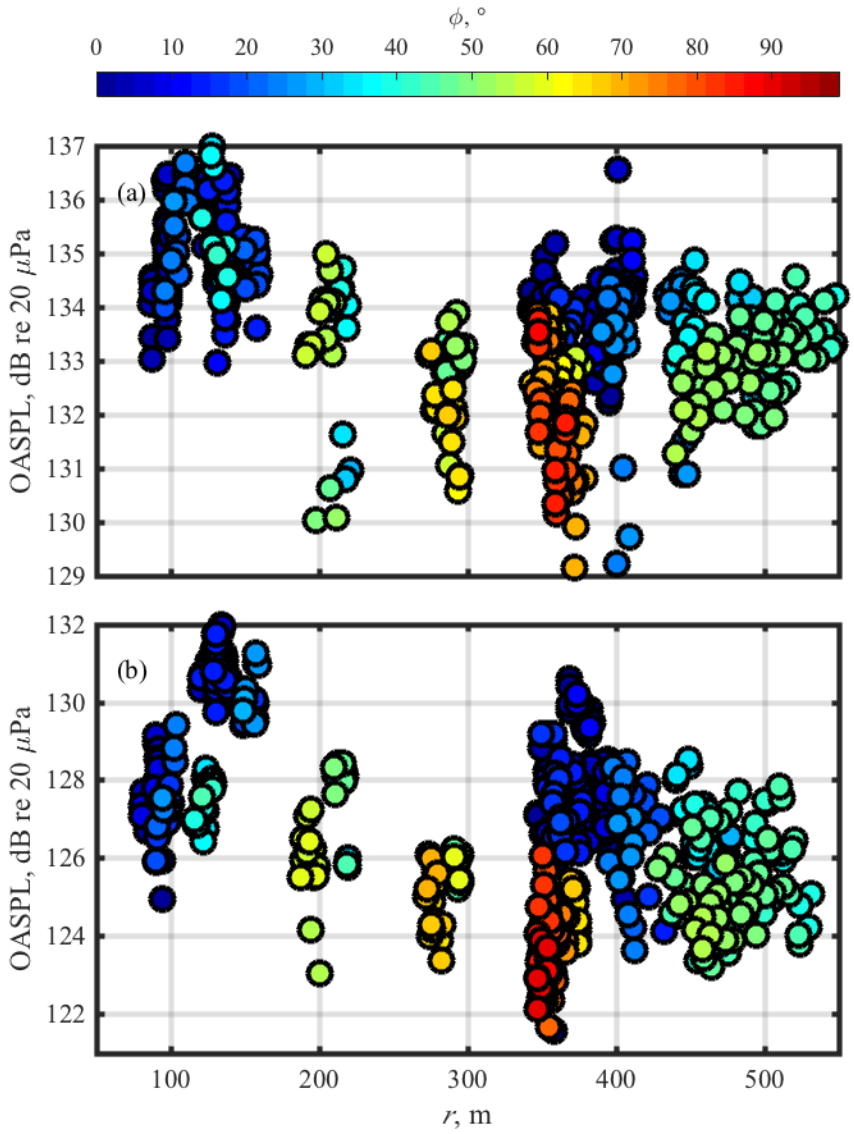


**Figure 7. OASPL at a polar angle of 120° plotted against measurement distance $r$ for flyover events at (a) 150% ETR and (b) 100% ETR.**

## V. Field Comparisons

While the comparison of OASPL and directivity describes some of the differences in the sound field between ground run-up and flyover measurements, more comparisons are needed to understand additional characteristics of the noise. However, as other metrics are not as easily corrected for distance as the OASPL, a different approach is needed to compare spectra and nonlinearity metrics, for example derivative skewness and ASF. In this section, a method of comparing the entire field is introduced, then comparisons are shown for OASPL, nonlinearity metrics, and spectra across the field of measurement for flyover events at 76 m.

### A. Method

As the aircraft flies near the measurement array, data are continuously collected at each microphone and the aircraft position is recorded every 0.1 s. Using the 0.05 s blocks mentioned in Section III.D, we can again calculate distance

and polar angle $\theta$ similar to process in Section IV.A. When the aircraft is flying at a height of 76 m, most of the microphones that can be compared with the ground run-up measurements are located near the flight path, meaning that we can assume any azimuthal variations are small for the microphones in question. With this assumption the aircraft paths, relative to each microphone, can be projected onto the same plane, giving data across a wide spatial range, at distances of less than 100 m from the source and outward. The data points associated with the closest flyover locations are shown in Figure 8, with each line of data points representing the aircraft flying near one of the microphones. With all the quantities of interest calculated at each point shown in Figure 8, the data can be interpolated and smoothed to recreate the spatial field for various quantities.

The method above relies on some assumptions for the field recreation to be valid. First, the field must be axisymmetric. Since the comparable ground run-up measurements are mainly within 300 m, the flyover microphones that contribute to the field recreation are all located near the flight path with an azimuthal angle near $\phi = 0$. These microphones near the flight path, though exhibiting slightly different directivities than at larger azimuthal angles, are consistent with each other and should provide reasonable map of each parameter over the area of interest. Another important point is that the data samples are 0.5 s long, meaning that the aircraft position varies considerably over the sample length. This uncertainty in aircraft position means that an average behavior is displayed.. A shorter time scale, such as 0.25 s, may lessen these effects, but uncertainty of the metrics, in particular the derivative skewness, rises considerably with a shorter time block. This method is first tested with OASPL, whose behavior is known due to the ease of correcting it for distance, and then applied to quantities that cannot be corrected for distance due to nonlinear propagation, such as spectra, derivative skewness, and ASF.

.



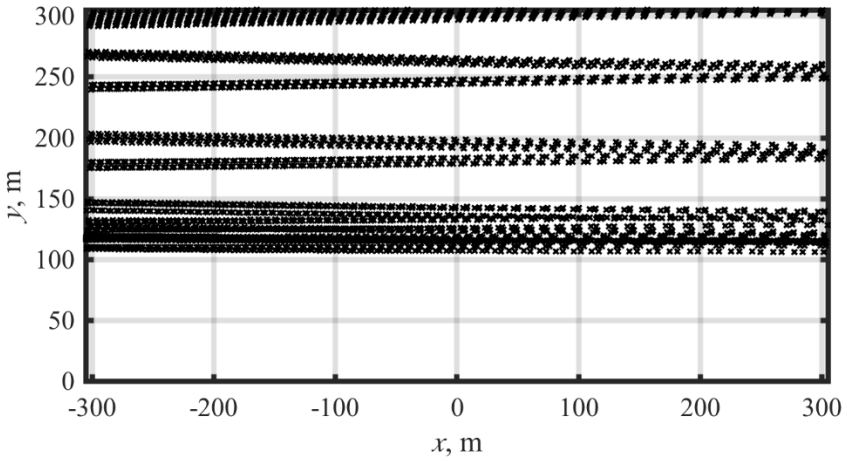


**Figure 8. Aircraft flight path relative to microphones for events with aircraft height of 76 m.**

## B. OASPL

To ensure that this method provides reliable results the recreated field is generated for a known quantity, such as the OASPL. The recreated OASPL from flyover measurements is compared with ground run-up results in Figure 9. The black dots shown in Figure 9(a) correspond to the microphone locations at 76 m, 152 m, and 305 m from the MARP for the ground run-up measurements. The recreated OASPL shown in Figure 9(b) agrees with the analysis above in Figure 4 and Figure **5**. An overall reduction in level is observed in the main lobe from Figure 9(a) to Figure 9(b), on the order of 3-4 dB, along with a shift forward in directivity roughly 5° and an increase in OASPL of roughly 3 dB in the forward direction. This helps establish the validity of the field recreation.

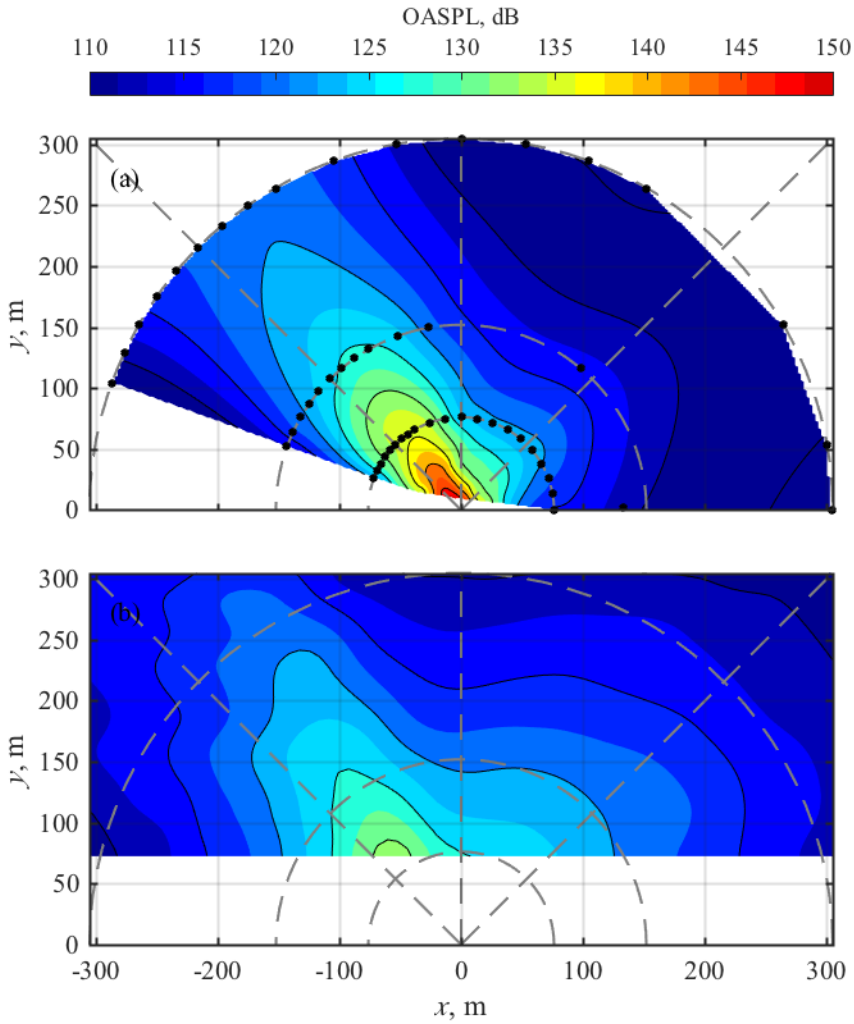


**Figure 9. Comparison of OASPL for (a) ground run-up and (b) flyover.**

## C. Spectra

While the OASPL may be the most important indicator of sound exposure, important physical questions about the nature of the source can be answered by investigating the spectra. However, nonlinear propagation and atmospheric absorption make it difficult to normalize the spectra to a specific distance as can be done with OASPL, so the spatial field must be recreated for each frequency. The flyover field recreation method results for one-third octave (OTO) spectra are shown at 76 m at 30°, 90°, and 125° in Figure 10(a), along with spectra from comparable ground run-up locations. Microphones from the ground run-up measurements were located at a height of 9.1 m, while the microphones used to recreate the flyover field were located at 0, 1.5, or 9.1 m above ground level. The same trends presented before are seen here as well—reduction in the maximum radiation region, seen as the decrease of 15 dB in the spectrum around 100 Hz at 125°, and a boost in the forward direction, seen as the increase of ~5 dB around 500 Hz at 30°. One interesting feature is that the peak frequencies are relatively unchanged between the two settings, in accordance with previous measurements.[2,6] Two peaks seen at 125° during ground run-up measurements are roughly 80-100 Hz and 315 Hz OTO bands. For the flyover measurements at the same locations, the peaks have different amplitudes, have no evidence of a Doppler shift in frequency, similar to expectations [2,5]. Similar behavior can be seen at both of the other angles shown, with peak frequency remaining stable between the two measurement scenarios. However, one difference that is noticeable is the increase in high-frequency energy in the forward direction

during flyover, as seen by the >20 dB increase at 10 kHz. The increased level in the forward direction during flyover likely drives an increase in waveform steepening due to nonlinear propagation effects, resulting in high-frequency energy not present in the forward direction during ground run-up. In the opposite case, the decrease in level at the peak frequency at 125° during flyover decreases the strength of the nonlinear propagation leading to less high-frequency energy due to a decrease in nonlinear propagation effects.

The increased importance of nonlinear propagation naturally brings up the question of how the spectrum changes as a function of angle. The relative gain, defined as the spectrum recreated from flyover events minus the measured spectrum from ground run-up, is shown in Figure 10(b). As expected, an overall increase in level happens in the forward direction, and high frequencies in particular see a dramatic boost due to nonlinear propagation. As the peak frequency is consistent between the two scenarios, the degree to which nonlinear propagation is important is dependent only on amplitude. An increase of 5 dB in the peak frequency at 30° then significantly increases the high frequency content due to nonlinear propagation during flyover. The opposite trend is seen from 90-130°, where the amplitude decreases at and below 300 Hz, which in turn leads to a decrease in high-frequency noise for flyover events.

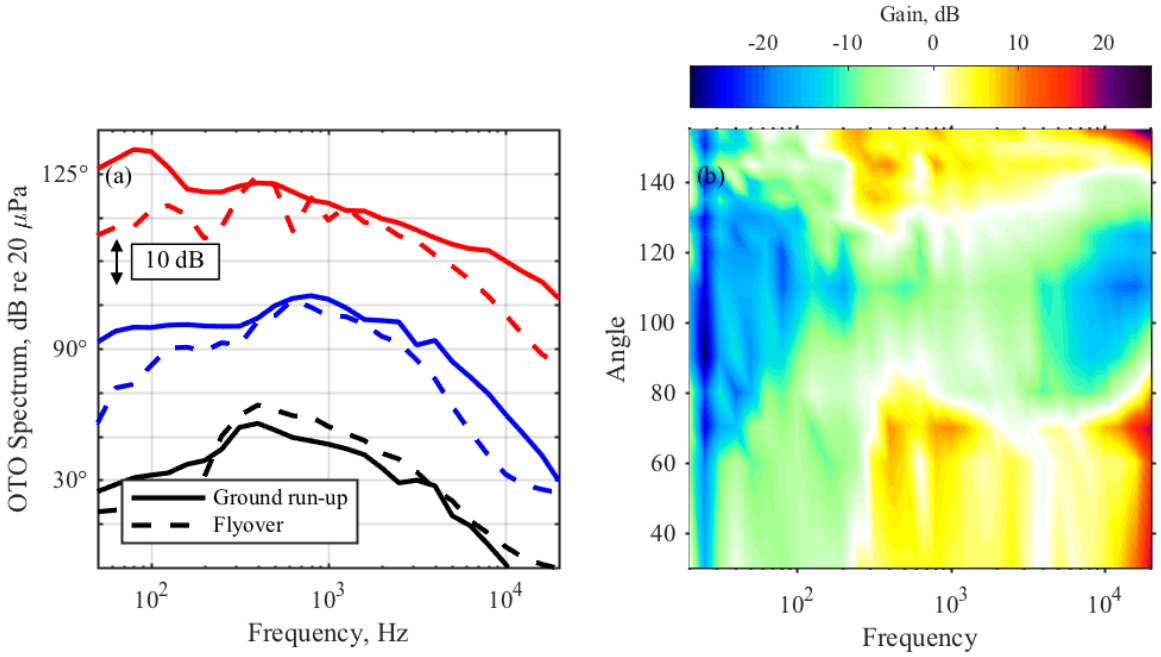


**Figure 10. (a) Comparison of spectra at a distance of 76 m between ground run-up and flyover at 150% ETR and (b) relative gain in level during flight.**

### D. Nonlinearity

The increase in high-frequency noise in the forward direction during flyover in Figure 10(a-b) is indicative of nonlinear propagation. If this is the case, it would be expected that the nonlinearity indicators introduced in Section III would have a relative increase from ground run-up to flyover in the forward direction, and a slight decrease in the maximum radiation region. Both these trends are seen in Figure 11. The derivative skewness, following the trends observed in Figure 9, shifts forwards, from peaking at 125° during ground run-up to peaking at 115° during flyover. The reduction in level in the maximum radiation region also leads to a decrease in derivative skewness levels, with maximum values at the 76 m radius arc reaching 13, rather than 17 as in ground run-up measurements. In the forward direction, however, there is a marked increase in derivative skewness for flyover, reaching a value of 13 at 30°. This high value indicates that, in contrast to the ground run-up scenario, significant shocks can be found in the forward direction during flyover measurements.

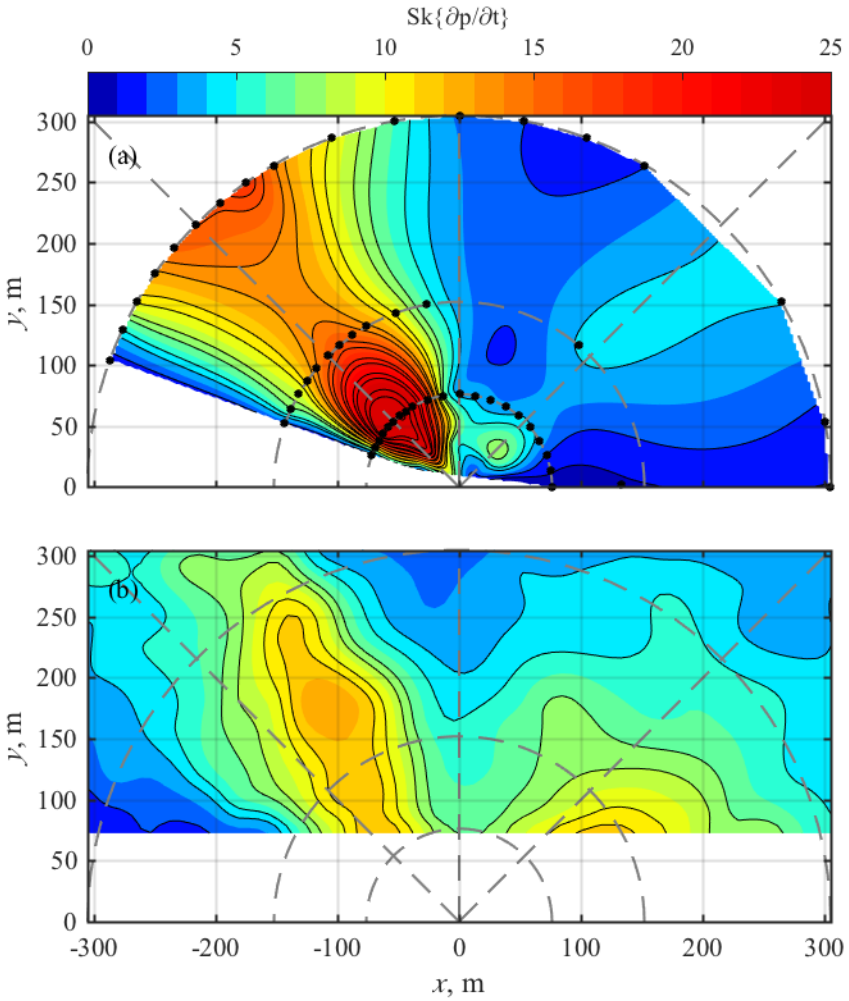


**Figure 11. Derivative skewness comparison between (a) ground run-up and (b) flyover.**

The trends seen in the derivative skewness are also evident in the ASF. As with derivative skewness and OASPL, the ASF directivity shifts forward, and lower values are seen in flyover in the maximum radiation region. The ASF values in the forward direction are significantly higher during flyover measurements. While the derivative skewness values in Figure 11(b) suggest the presence of shocks mainly between 20° and 45°, the ASF is higher in all forward directions. This increase indicates that although shocks may not be a significant feature of the waveform between 45° and 90°, nonlinear propagation is still a factor, leading to a steeper overall waveform.

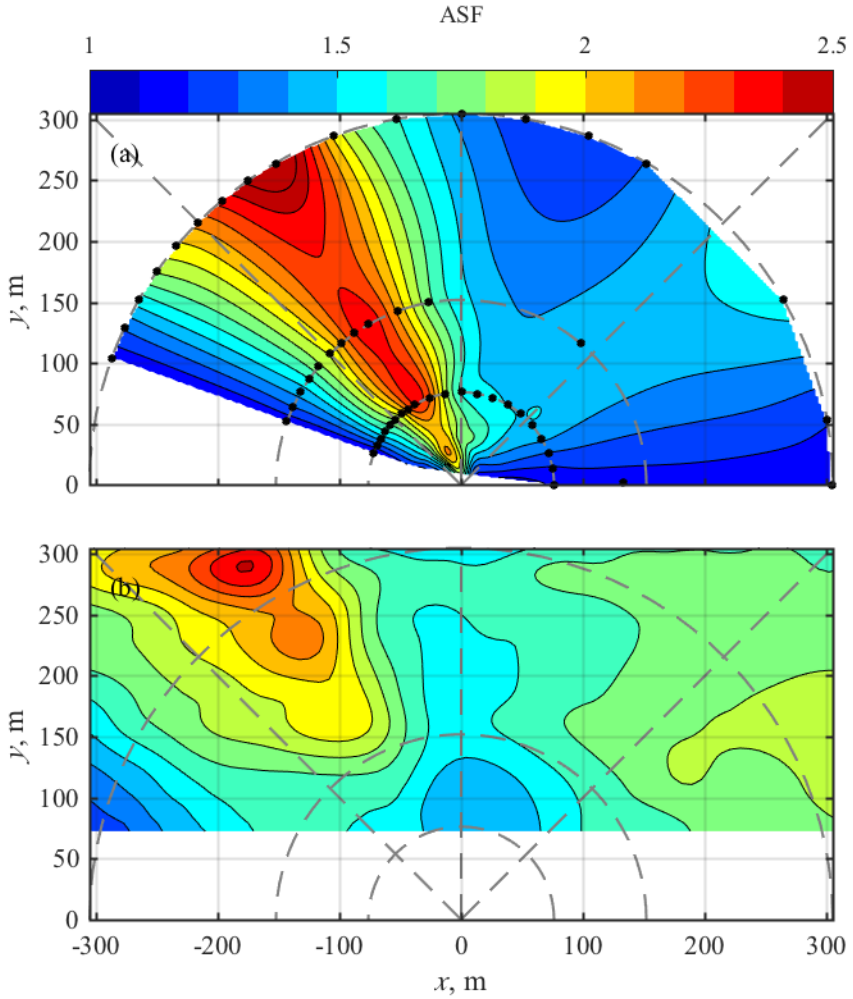


**Figure 12. ASF comparison between (a) ground run-up and (b) flyover.**

## VI.Results at other engine conditions

### A. OASPL

Flight effects at 150% ETR are consistent with prior work, and it is reasonable to expect that those effects are seen at other engine powers as well. Figure 13 shows the OASPL comparison between ground run-up and flyover effects for (a) 75% ETR and (b) 100% ETR at an aircraft height of 76 m. The expected trends are seen here, but the effects are even more exaggerated than at 150% ETR in Figure 4. In particular, at 75% ETR the OASPL in the maximum radiation region decreases from 131 to 125 dB at a distance of 76 m, while in the forward direction the OASPL increases by 10 dB, from 112 dB to 122 dB. These changes are substantial as the noise in the forward direction during flyover is comparable to the noise in the backward direction. The changes due to flyover at 100% ETR are more noticeable than at 150% ETR, but less dramatic than those seen at 75% ETR. In the maximum radiation region, OASPL is decreased by 3 dB, while forward radiation is increased by 5 dB. The increased importance of flight effects for lower engine conditions is likely due to the fact that although exhaust velocity changes drastically between the engine conditions, aircraft speed is comparable between the three measurements. This means that aircraft speed is a

more significant fraction of exhaust velocity at lower engine conditions, leading to an increase in importance of flight effects. The significant changes in OASPL in Figure 13 are likely to lead to noticeable differences in nonlinearity and shock content between ground run-up and flyover situations.

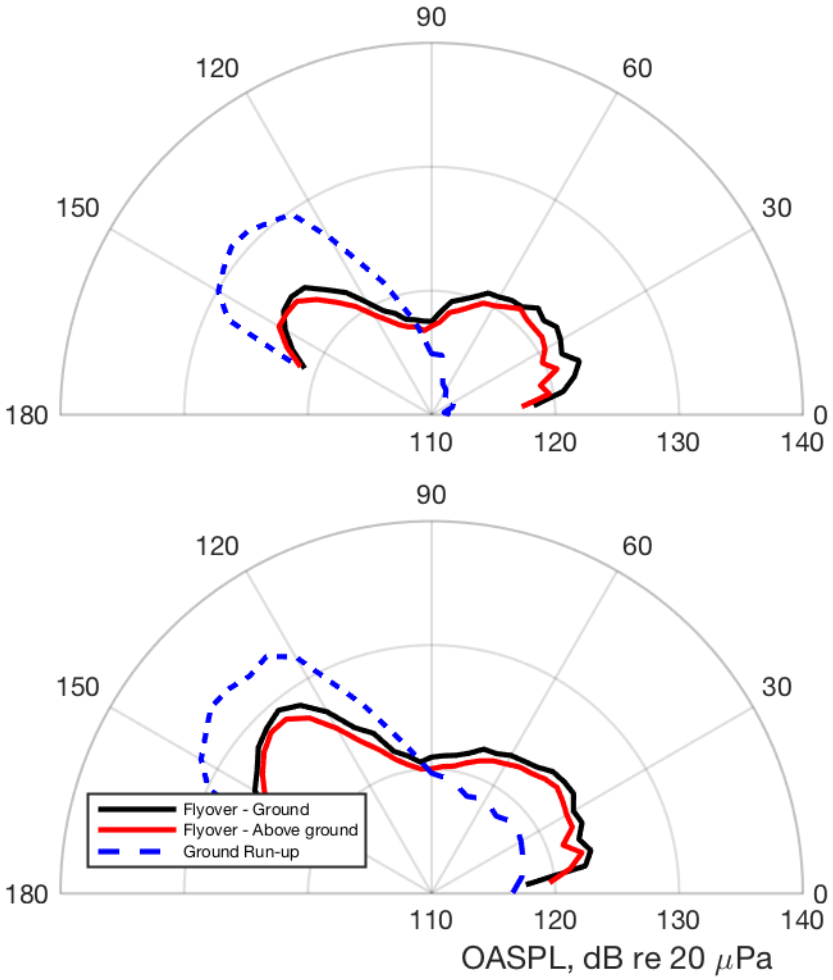


**Figure 13. Average flyover directivity at an aircraft height of 76 m compared with ground run-up at (a) 75% ETR and (b) 100% ETR.**

### B. Nonlinearity comparisons

In the comparisons of nonlinearity metrics at 150% in Figure 11 and Figure 12, it was observed that the decrease in OASPL in the peak radiation direction led to a slight decrease in shock content, while the increase in the forward direction led to an increase in shock content, as would be expected. Since the changes seen in OASPL are more significant at 75% and 100% ETR, the changes in nonlinearity metrics should also be more noticeable. This expectation is born out in Figure 14 and Figure 15; the derivative skewness maps are compared between ground run-up and flyover for 75% ETR in Figure 14(a) and (b) and 100% ETRvin Figure 15 (a) and (b). The reduction in OASPL

in the maximum radiation region does lead to a decrease in derivative skewness in that direction. In the ground run-up scenario at 75% ETR, derivative skewness values peak at 20 at a distance of 76 m from the MARP, while derivative skewness values in Figure 14(b) peak at a value of $\mathrm{Sk}\{\partial p/\partial t\} = 7$. However, the forward direction does increase in derivative skewness, from values of $\mathrm{Sk}\{\partial p/\partial t\} < 1$ to values of $\mathrm{Sk}\{\partial p/\partial t\} > 6$, indicating the presence of significant shocks in the forward direction for the 75% ETR flyover events that were absent during ground run-up. Similar changes are seen at 100% ETR, with a significant decrease in derivative skewness in the maximum radiation region and an increase in the forward direction during flyover, albeit the increase in the forward direction is not as significant at 100% ETR as it is at 75% ETR. Interestingly, the derivative skewness levels in the forward direction are similar at 75% and 100% ETR, which could be expected as the OASPL in the forward direction at 75% is within 1-2 dB of the OASPL at 100%.

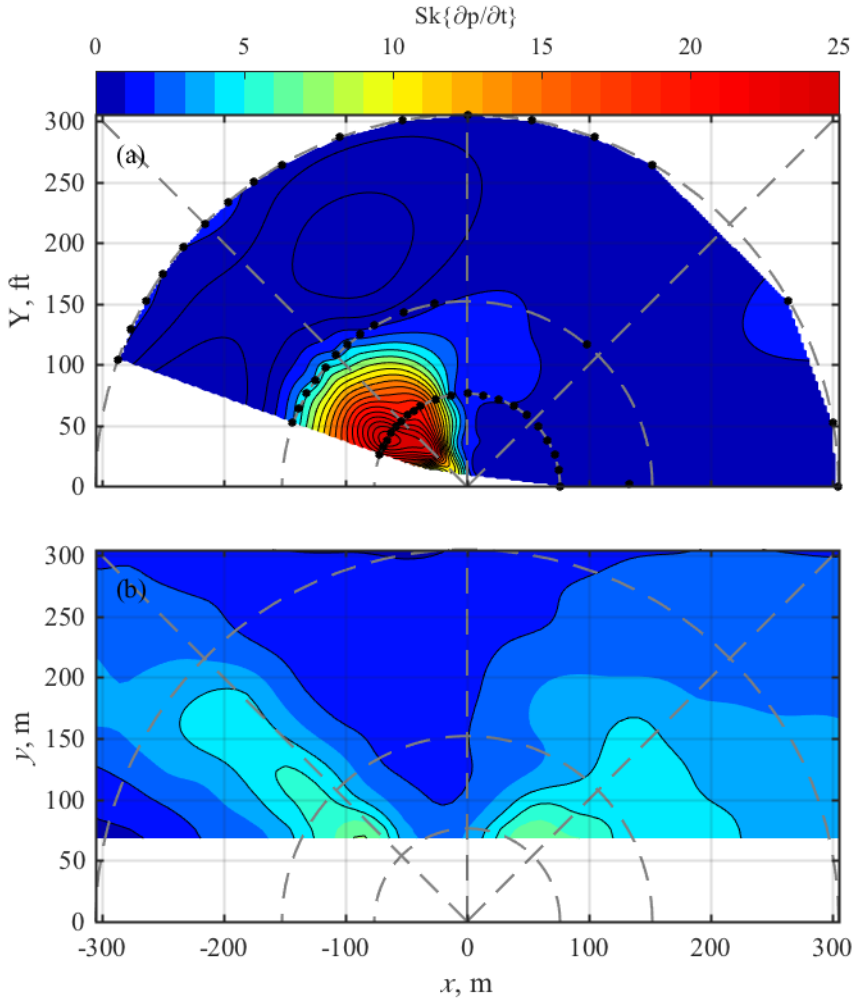


**Figure 14. Derivative skewness at 75% ETR for (a) ground run-up and (b) flyover.**

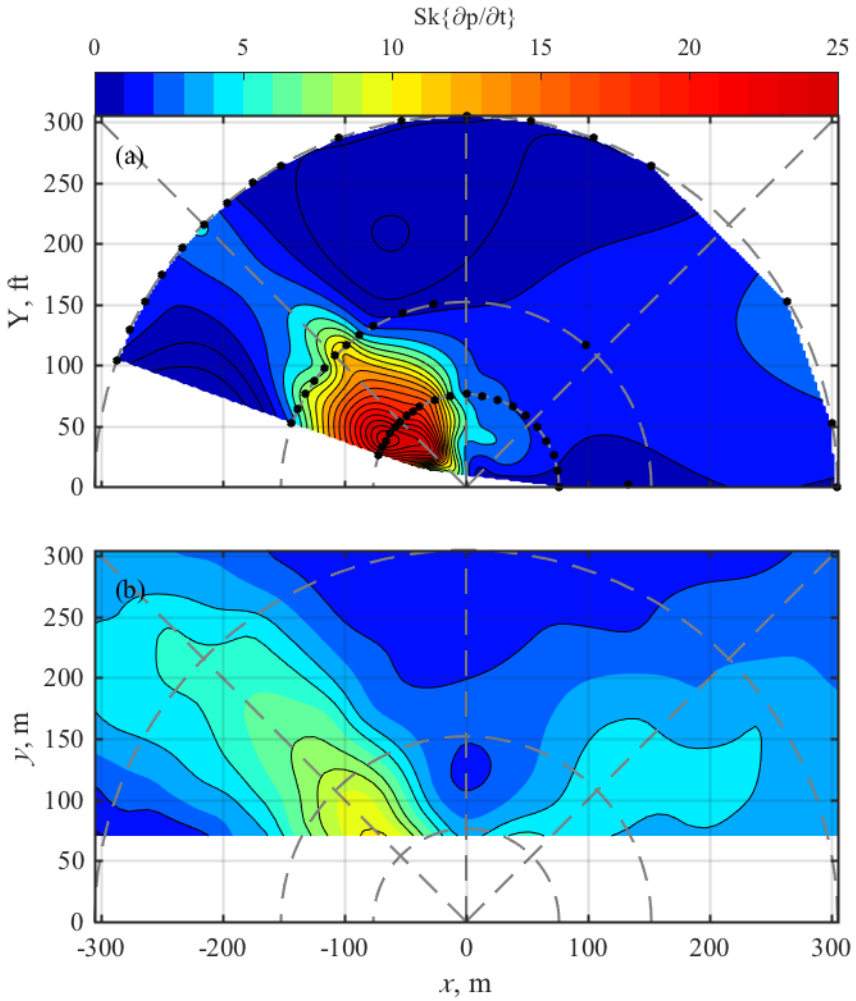


**Figure 15. Derivative skewness at 100% ETR for (a) ground run-up and (b) flyover.**

The ASF again confirms the expected behavior of nonlinear propagation and shock content. The ASF is shown in ground run-up and flyover experiments for 75% ETR in Figure 16(a) and (b) and 100% ETR in Figure 17(a) and (b). Once again a decrease in the nonlinearity indicator is seen in the maximum radiation region associated with the decrease in OASPL due to flight effects, though the decrease in ASF is not as significant as that of derivative skewness. An increase in ASF is also seen in the forward direction in both cases, and again values in the forward direction during flyover are comparable between 75% ETR and 100% ETR.

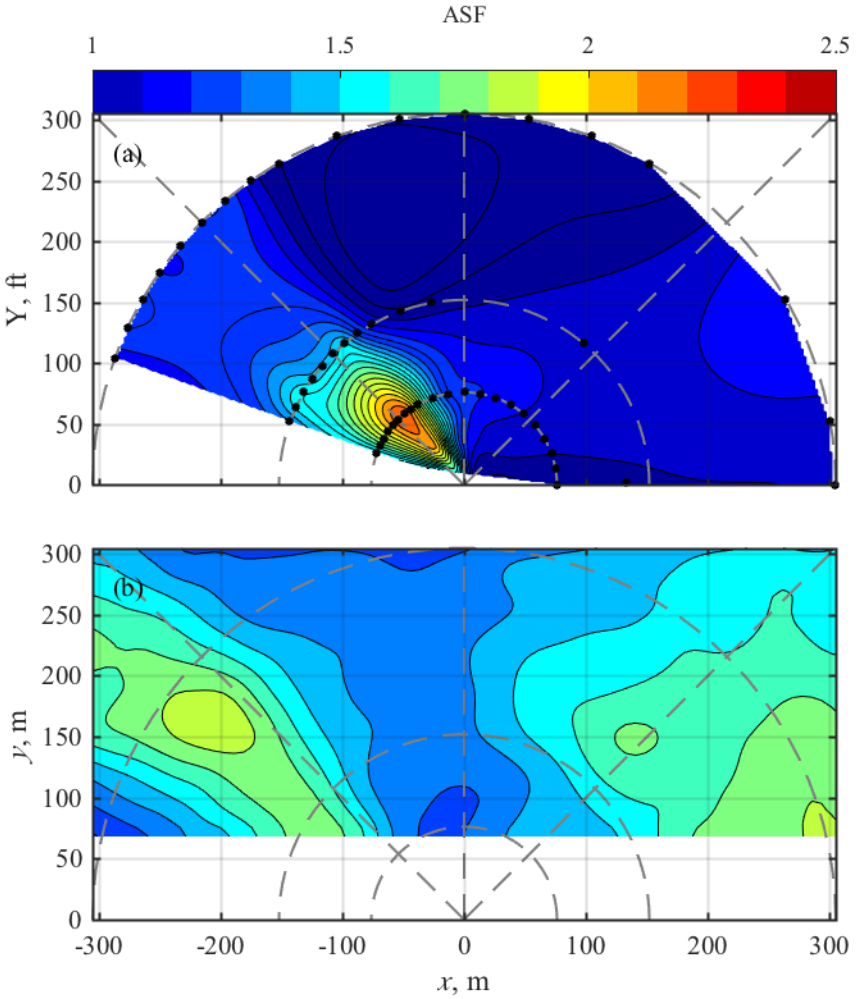


**Figure 16. ASF at 75% ETR for (a) ground run-up and (b) flyover.**

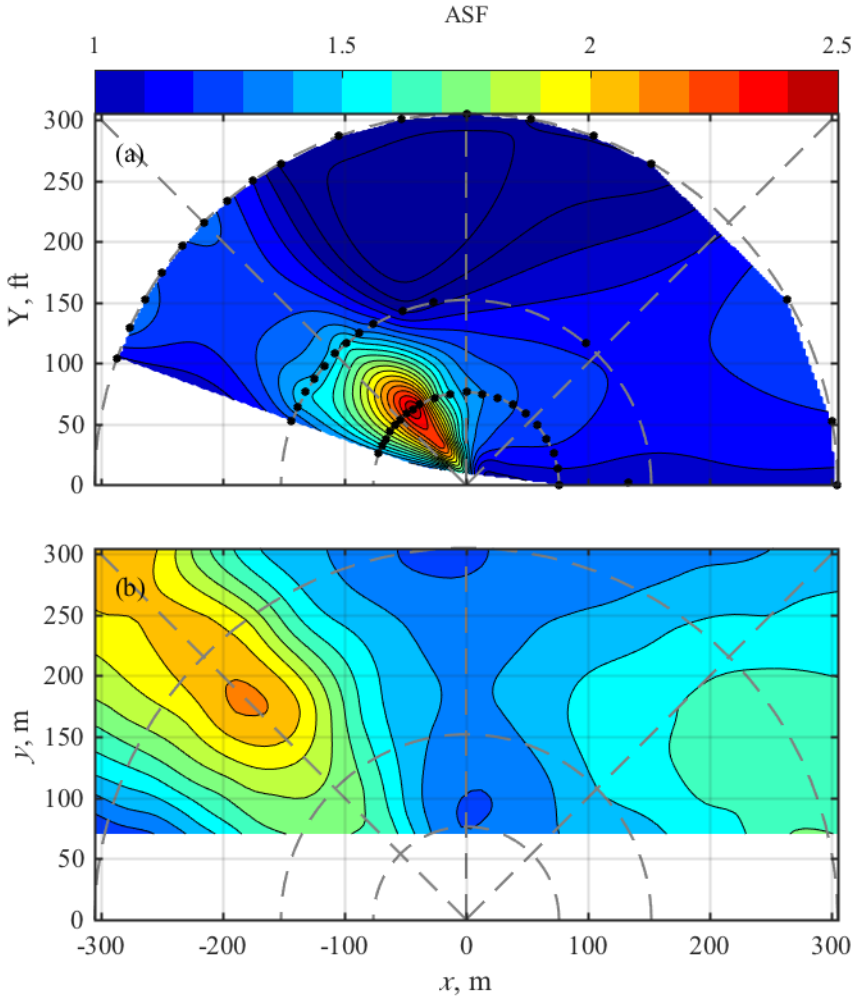


**Figure 17. ASF at 100% ETR for (a) ground run-up and (b) flyover.**

## VII. Conclusions and Future Work

Understanding the changes in jet noise sources due to forward flight is an essential link in effective planning for jet noise exposure around military bases. Directivity, OASPL, spectra, and nonlinearity indicators have been compared between ground run-up and flyover measurements. In line with previous studies for analytical and model-scale results and predictions, the OASPL changes in three distinct ways due to forward flight effects: The maximum radiation region shifts forwards, the OASPL in this region decreases slightly, and the levels in the forward direction increase. The relative changes in level result in lower and higher importance of nonlinear propagation, which result in slightly lower high-frequency levels at peak radiation angles and a significant increase in high-frequency levels in the forward direction, which are due to a reduction and increase, respectively, in energy gain due to nonlinear propagation. While significant shocks are still found in the maximum radiation region during flight, shocks are also found in the forward direction at angles of less than 45°, and the increase in level in the forward direction results in an overall steeper waveform.

The trends expected from prior work are even more evident at lower engine conditions. The increase in forward radiation is especially dramatic at 75% ETR, with a 10 dB increase over ground run-up measurements. The increase in OASPL in the forward direction does result in nonlinear propagation and shock formation at 75% and 100% ETR, but the decrease in the maximum radiation region results in a significant decrease in derivative skewness, as well as a small decrease in ASF. Overall, the trends seen here show that the flight effects may create significant shock content in areas where such content is absent during ground run-up measurements.

## Appendix A. Effect of block size.

One issue with flyover measurements is the short integration times associated with measurements when the aircraft is flying close to the microphones at a high speed.[2] This problem is apparent when trying to assess directivity. The constant movement of an aircraft, often at speeds of hundreds of meters per second, means that the period of time at which the aircraft is at a relatively constant angle is very short, even when measuring at distances of almost 100 m from the source. However, using a short integration time can introduce noise. To illustrate these effects, Figure A1 shows the directivity curves of Figure 4 with three different integration times: (a) 0.1 s, (b) 0.25 (s), (c) 0.5 s for a single flyover event. The variation seen in Figure A1(a) is due to the short block size of 1/10 s, and the variation decreases significantly with block sizes of 0.25 s and 0.5 s. However, directivity estimates begin to be altered with longer block sizes. To give context on the length of time that is being considered, the dots in Figure 8 show the aircraft position every 0.1 s, meaning that over 0.5 s the aircraft can travel almost 100 m.

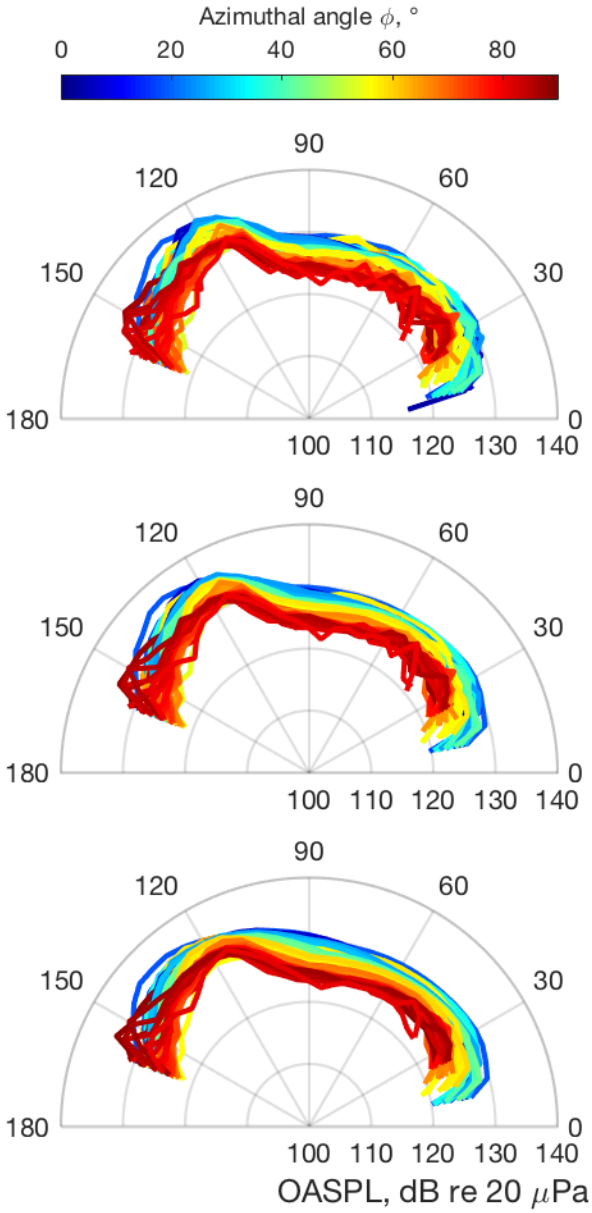


**Figure A1. Polar directivity during flyover events for block sizes of (a) 0.1 s, (b) 0.25 s, and (c) 0.5 s.**

When the directivity patterns shown in Figure A1 are averaged over all microphone locations, much of the noise associated with short integration times is smoothed out. However, the false directivity patterns due to longer integration times persist, as shown in Figure A2. For this reason, a block size of 0.1 s was chosen for the analyses in this paper, given that the correct behavior averaged over events is of more importance for the sake of comparison with ground run-up.

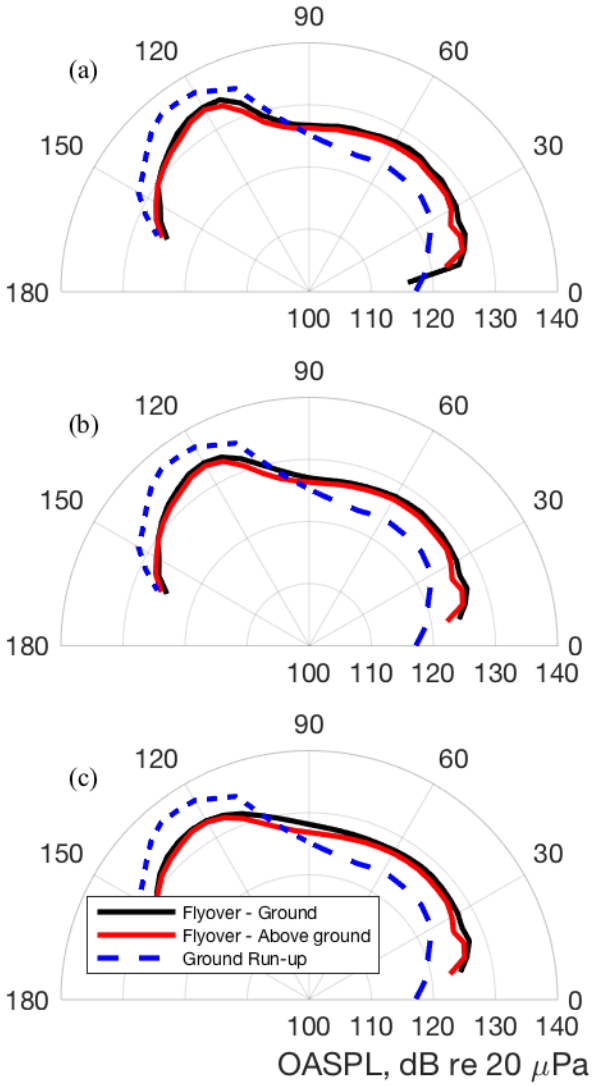


**Figure A2. Average polar directivity during flyover events for block sizes of (a) 0.1 s, (b) 0.25 s, and (c) 0.5 s.**

## Acknowledgments

The authors would like to gratefully acknowledge funding for the measurements, provided through the F-35 Program Office and Air Force Research Labs. (Distribution A - Approved for Public Release; Distribution is Unlimited. F-35 PAO Cleared 04/23/2018; JSF18-414) The authors would also like to thank members of Naval Air Systems Command and Wyle Laboratories for their assistance in both the ground run-up and flyover measurements. B.O. Reichman was funded through an appointment to the Student Research Participation Program at the U.S. Air Force Research Laboratory, 711th Human Performance Wing, Human Effectiveness Directorate, Warfighter Interface Division, Battlespace Acoustics Branch administered by the Oak Ridge

Institute for Science and Education through an interagency agreement between the U.S. Department of Energy and USAFRL.

## References

1 Hoch, R., and Berthelot, M. "Use of the bertin aérotrain for the investigation of flight effects on aircraft engine exhaust noise," *Journal of Sound and Vibration* Vol. 54, No. 2, 1977, pp. 153-172.

2 Drevet, P., Duponchel, J., and Jacques, J. "The effect of flight on jet noise as observed on the Bertin Aérotrain," *Journal of Sound and Vibration* Vol. 54, No. 2, 1977, pp. 173-201.

3 Michalke, A., and Michel, U. "Prediction of jet noise in flight from static tests," *Journal of Sound and Vibration* Vol. 67, No. 3, 1979, pp. 341-367.

4 Veltin, J., Day, B. J., McLaughlin, D. K., "Forward flight effect on small scale supersonic jet acoustics," AIAA Paper 2010-3924, 2010.

5 Michel, U. "Prediction of jet mixing noise in flight from static tests," AIAA paper 2016-2807, 2016.

6 Viswanathan, K., and Czech, M. "Measurement and modeling of effect of forward flight on jet noise," *AIAA Journal* Vol. 49, No. 1, 2011, pp. 216-234.

7 Blackstock, D. T. "Nonlinear propagation of jet noise," *Third Interagency Symposium on University Research in Transportation Noise*. U.S. Department of Transportation, University of Utah, Salt Lake City, Utah, 1975, pp. 389-397.

8 Gee, K. L., Sparrow, V. W., Gabrielson, T. B., and Atchley, A. A. "Nonlinear modeling of F/A-18E noise propagation," *AIAA Paper* 2005-3089, 2005.

9 Morfey, C. L., and Howell, G. P. "Nonlinear propagation of aircraft noise in the atmosphere," *AIAA Journal,* Vol. 19, No. 8, 1981, pp. 986-992.

10 Baars, W. J., Tinney, C. E., and Wochner, M. S. "Nonlinear Noise Propagation from a Fully Expanded Mach 3 Jet," *AIAA paper* Vol. 2012, 2012, p. 1177. doi:10.2514/6.2012-1177

11 Gee, K. L., Atchley, A. A., Falco, L. E., and Shepherd, M. R. "Nonlinearity analysis of model-scale jet noise," *19th International Symposium on Nonlinear Acoustics*. Vol. 1474, AIP Publishing, Tokyo, Japan, 2012, pp. 307-310.

12 Petitjean, B. P., Viswanathan, K., and McLaughlin, D. K. "Acoustic pressure waveforms measured in high speed jet noise experiencing nonlinear propagation," *International Journal of Aeroacoustics* Vol. 5, No. 2, 2006, pp. 193-215.

13 Ffowcs-Williams, J. E. S., J.; Virchis, V.J. "'Crackle': an annoying component of jet noise," *Journal of Fluid Mechanics* Vol. 71, No. 2, 1975, pp. 251-271.

14 Gee, K. L., Sparrow, V. W., James, M. M., Downing, J. M., Hobbs, C. M., Gabrielson, T. B., and Atchley, A. A. "The role of nonlinear effects in the propagation of noise from high-power jet aircraft," *The Journal of the Acoustical Society of America* Vol. 123, No. 6, 2008, pp. 4082-4093.

15 McInerny, S., Gee, K. L., Dowing, M., and James, M. "Acoustical nonlinearities in aircraft flyover data," AIAA paper 2007-3654, 2007.

16 Reichman, B. O., Gee, K. L., Neilsen, T. B., Downing, J. M., James, M. M., Wall, A. T., and McInerny, S. A., "Characterizing acoustic shocks in high-performance jet aircraft flyover noise," *The Journal of the Acoustical Society of America* Vol. 143, No. 3, 2018, pp. 1355-1365.

17 James, M. M., Salton, A. R., Downing, J. M., Gee, K. L., Neilsen, T. B., Reichman, B. O., McKinley, R. L., Wall, A. T., and Gallagher, H. L. "Acoustic Emissions from F-35 Aircraft during Ground Run-Up," *AIAA paper* Vol. 2015, 2015, p. 2375.

18 Gee, K. L., Sparrow, V. W., Atchley, A. A., and Gabrielson, T. B. "On the perception of crackle in high-amplitude jet noise," *AIAA Journal* Vol. 45, No. 3, 2007, pp. 593-598.

19 McInerny, S. A. "Launch vehicle acoustics. II-Statistics of the time domain data," *Journal of aircraft* Vol. 33, No. 3, 1996, pp. 518-523.

20 Reichman, B. O., Muhlestein, M. B., Gee, K. L., Neilsen, T. B., and Thomas, D. C. "Evolution of the derivative skewness for nonlinearly propagating waves," *The Journal of the Acoustical Society of America* Vol. 139, No. 3, 2016, pp. 1390-1403. doi: 10.1121/1.4944036

21 Gee, K. L., Neilsen, T. B., Wall, A. T., Downing, J. M., James, M. M., and McKinley, R. L. "Propagation of crackle-containing jet noise from high-performance engines," *Noise Control Engineering Journal* Vol. 64, No. 1, 2016, pp. 1-12.

22 Muhlestein, M. B., Gee, K. L., Neilsen, T. B., and Thomas, D. C. "Evolution of the average steepening factor for nonlinearly propagating waves," *The Journal of the Acoustical Society of America* Vol. 137, No. 2, 2015, pp. 640-650.

23 Gallagher, J. "The effect of non-linear propagation in jet noise," *AIAA, Aerospace Sciences Meeting*. 1982.

24 W. J. Baars and C. E. Tinney, " Shock-structures in the acoustic field of a Mach 3 jet with crackle," J. Sound and Vib. **12**, 2539-2553 (2014).

25 K. L. Gee, T. B. Neilsen, J. M. Downing, M. M. James, R. L. McKinley, R. C. McKinley, and A. T. Wall, "Near-field shock formation in noise propagation from a high-power jet aircraft," J. Acoust. Soc. Am. **133**, EL88-EL93 (2013).

26 Zwieback, E. "Flyover noise testing of commercial jet airplanes," *Journal of Aircraft* Vol. 10, No. 9, 1973, pp. 538-545.

27 Howell, G., Bradley, A., McCormick, M., and Brown, J. "De-dopplerization and acoustic imaging of aircraft flyover noise measurements," *Journal of Sound and Vibration* Vol. 105, No. 1, 1986, pp. 151-167.

28 Pott-Pollenske, M., Dobrzynski, W., Buchholz, H., Guérin, S., Saueressig, G., and Finke, U. "Airframe noise characteristics from flyover measurements and predictions," *AIAA paper* 2006-2567. (2006)